Published in final edited form as:
Mol Cell. 2008 December 5; 32(5): 641–651. doi:10.1016/j.molcel.2008.11.014.

Role of SERCA1 Truncated Isoform in the Proapoptotic Calcium Transfer from ER to Mitochondria during ER Stress

Mounia Chami[1,2,5,*], **Bénédicte Oulès**[1,2,5], **György Szabadkai**[1,2,3], **Rachida Tacine**[1,2], **Rosario Rizzuto**[4], and **Patrizia Paterlini-Bréchot**[1,2]

[1]INSERM U 807, Paris F-75015, France

[2]Université Paris Descartes, Paris F-75015, France

[3]Department of Cell and Developmental Biology, University College London, Gower Street, WC1 6BT London, UK

[4]Department of Experimental and Diagnostic Medicine, Section of General Pathology, Interdisciplinary Center for the Study of Inflammation (ICSI) and ER-GenTech, University of Ferrara, 44100 Ferrara, Italy

SUMMARY

Among the new players at the endoplasmic reticulum (ER)-mitochondria interface regulating interorganelle calcium signaling, those specifically involved during ER stress are not known at present. We report here that the truncated variant of the sarcoendoplasmic reticulum Ca^{2+}-ATPase 1 (S1T) amplifies ER stress through the PERK-eIF2α-ATF4-CHOP pathway. S1T, which is localized in the ER-mitochondria microdomains, determines ER Ca^{2+} depletion due to increased Ca^{2+} leak, an increased number of ER-mitochondria contact sites, and inhibition of mitochondria movements. This leads to increased Ca^{2+} transfer to mitochondria in both resting and stimulated conditions and activation of the mitochondrial apoptotic pathway. Interestingly, S1T knockdown was shown to prevent ER stress, mitochondrial Ca^{2+} overload, and subsequent apoptosis. Thus, by bridging ER stress to apoptosis through increased ER-mitochondria Ca^{2+} transfer, S1T acts as an essential determinant of cellular fate.

INTRODUCTION

Calcium stored in the endoplasmic reticulum (ER) is crucial for posttranslational processing, folding, and export of proteins synthesized on ER-associated ribosomes, as well as for calcium (Ca^{2+}) signaling (Berridge et al., 2000). Accumulation of unfolded proteins in the ER lumen and ER Ca^{2+} depletion induce ER stress, eliciting unfolded protein response (UPR), which is mediated by three pathways under the control of ER resident molecular "sentinels": IRE1α (inositol-requiring transmembrane kinase and endonuclease 1α), PERK (protein kinase-like ER kinase), and ATF6 (activation of transcription factor 6) (Schroder and Kaufman, 2005). These sensors activate specific transcription factors (such as spliced XBP1, ATF6, and Activating Transcription Factor 4 [ATF4]), triggering the expression of UPR-related genes (such as C/EBP homologous protein [*CHOP*] and Glucose-Regulated Protein 78 [*GRP78*])

*Correspondence: mounia.chami@inserm.fr.
[5]These authors contributed equally to this work

SUPPLEMENTAL DATA The Supplemental Data include Supplemental Experimental Procedures, Supplemental References, seven figures, and five tables and can be found with this article online at http://www.cell.com/molecular-cell/supplemental/S1097-2765(08)00809-5.

and determining the cellular fate. By reducing misfolded protein levels, UPR promotes cell survival, while unmitigated ER stress triggers apoptotic death (Boyce and Yuan, 2006). ER stress-dependent apoptosis was reported to be mediated by murine caspase-12/human caspase-4 and activation of proapoptotic members of the Bcl-2 family (i.e., Bax, Bak, Bim, Puma, etc.) and of CHOP (Hetz et al., 2006; Li et al., 2006; Puthalakath et al., 2007; Szegezdi et al., 2006).

Calcium has been studied for a long time as a regulator of apoptosis following its physiological or physiopathological release from the ER (Rizzuto et al., 2003). Recently, ER-mitochondria physical interactions have drawn attention as pivotal routes for Ca^{2+} transfer from the ER to the mitochondria, mediating interorganelle Ca^{2+} signaling and potentially leading to mitochondrial Ca^{2+} overload and apoptotic cell death (Pizzo and Pozzan, 2007). A few proteins have been involved in the ER-mitochondria contacts, including the ER membrane resident Ca^{2+}-releasing channel, the inositol 1,4,5-triphosphate receptor (IP_3R); an outer mitochondrial membrane resident protein, the voltage-dependent anion channel (VDAC); the sorting protein PACS-2; and the molecular chaperones grp75 and Sigma-1R (Hayashi and Su, 2007; Pizzo and Pozzan, 2007; Simmen et al., 2005; Szabadkai et al., 2006).

In ER stress conditions, mitochondrial Ca^{2+} overload has been shown to be involved in mitochondrial apoptosis (Deniaud et al., 2008; Ferreiro et al., 2008). However, the molecular mechanism allowing increased Ca^{2+} transfer from the ER to the mitochondria under ER stress is not completely understood.

Active Ca^{2+} transport into the ER from the cytosol is ensured by sarcoendoplasmic reticulum calcium ATPases (SERCAs), creating a high [Ca^{2+}] gradient between the cytosol and the ER lumen (~0.1 μM versus ~400 μM). SERCAs are encoded by three homologous genes (*SERCA1-SERCA3*) giving rise to 11 alternative spliced isoforms (Bobe et al., 2005; Vangheluwe et al., 2005; Zhang et al., 1995). We have previously described a SERCA1 variant (S1T) characterized by exon 11 splicing, encoding a C-terminally truncated protein unable to pump Ca^{2+} and which induces ER Ca^{2+} leak (Chami et al., 2001).

In this work, we provide evidence that S1T is induced upon ER stress and acts by increasing Ca^{2+} transfer from the ER to mitochondria. Thus, S1T is revealed as an ER stress protein directly involved in Ca^{2+}-dependent mitochondrial apoptosis.

RESULTS

S1T Induction Is Involved in ER Stress Response

First, we investigated the role of S1T in ER stress induction. Unlike full-length SERCA1 isoform, overexpression of S1T native protein (S1T) as well as S1T-myc-His (S1T-myc-His) or GFP (S1T-GFP)-fused proteins in HeLa cells induced a set of ER stress proteins (Figures 1A and S1A and S1B [available online]).

Analysis of endogenous S1T protein expression under various ER stress conditions revealed a parallel induction of S1T and of ER stress markers in HeLa cells upon ER Ca^{2+} depletion by thapsigargin (TG) or tert-butylhydroquinone (TBU), as well as after buffering extracellular Ca^{2+} by EGTA or blocking either ER to Golgi protein transport by brefeldin A (BFA) or N-linked glycosylation by tunicamycin (TUN) (Figure 1B). ER stress-induced S1T expression was observed in a series of human-derived transformed cell lines in a dose-dependent manner (Figures S1C and S1D). A similar extent of S1T and of ER stress markers expression was observed upon ER stress induction and S1T ectopic expression (Figure S1E). Interestingly, the full-length SERCA1 isoform was not induced upon BFA treatment (Figure S1F), thus demonstrating the specific induction of S1T isoform by ER stressors.

Importantly, induction of endogenous S1T was also observed in a physiopathological ER stress model, the hepatitis C virus "replicon," i.e., HuH7 cell line stably expressing the HCV genome (Benali-Furet et al., 2005) (Figure 1C).

All in all, the above results suggest an amplifying role of S1T in ER stress signaling. Indeed, transfection of HeLa cells with an RNAi blocking the expression of endogenous S1T ($S1T_{RNAi}$) efficiently reduced the expression of P-eIF2α as well as that of GRP94 and CHOP in BFA-induced ER stress and that of GRP94 in the HCV replicon model (Figures 1D and 1E). Since $S1T_{RNAi}$ transfection efficiency averaged 40% in HeLa cells (Figure S2A), we assumed that S1T is a key component of ER stress induction and amplification in these models. As controls we showed that (1) a control RNAi ($Control_{RNAi}$) did not interfere with BFA-induced expression of S1T and ER stress markers (Figure 1D), and (2) neither $S1T_{RNAi}$ nor $Control_{RNAi}$ modified the expression of proteins involved in Ca^{2+} homeostasis (SERCA2b, IP_3R, VDAC) and in ER stress (GRP78, P-eIF2α) in nontreated cells (Figure S2B).

S1T Is Induced by ER Stress through the PERK-eIF2α-ATF4 Pathway

To elucidate the mechanisms underlying S1T induction upon ER stress, kinetic studies of the expression of S1T, as well as of known ER stress proteins, were performed in BFA-treated HeLa cells. S1T expression was shown to occur in a biphasic manner: a rapid increase after 40 min of treatment following eIF2α phosphorylation and ATF4 expression (Figure 2A, left panel), a transient decline between 2 hr and 8 hr, and a pronounced reinduction at 10 hr preceded by eIF2α phosphorylation, ATF6 cleavage, and ATF4 and CHOP expression and accompanied by an increase of GRP78 and GRP94 protein level (Figure 2A, right panel). These data suggest that the initial induction of S1T expression might occur through ATF4 activation, while the late reinduction might involve the ATF4, ATF6, and CHOP transcription factors. Comparative promoter analysis of human *SERCA1* gene and its orthologs revealed the presence of (1) an ATF4-responsive element (ATF/Cre) analogous to those previously described in different ER stress genes (*GRP78* and *GADD34*) (Luo et al., 2003) (Figure 2B, upper panel) and (2) a CHOP-responsive element responsible for the induction of ER and mitochondrial stress genes (Ohoka et al., 2005)(Figure 2B, lower panel). However, no conserved ATF6-responsive element (ERSE) (Yoshida et al., 1998) was found, arguing against the direct implication of ATF6 in the induction of S1T upon ER stress.

We then explored the functional activity of the identified responsive elements by using electrophoretic mobility shift assay (EMSA). An increase of DNA/protein complexes was observed with human *SERCA1* ATF/Cre probe upon 40 min of BFA treatment, and with human CHOP probe upon 20 hr of BFA treatment. Similar DNA/protein complexes were observed with the murine *GADD34* ATF/Cre and the human *Cpn60/10* CHOP probes used as positive controls for ATF4 and CHOP binding, respectively (Figure 2C).

We then demonstrated that ATF4 and CHOP transcription factors belong to the protein complexes respectively bound to *SERCA1* ATF/Cre and CHOP elements upon BFA treatment by using DNA-protein pull-down assay followed by western blot analysis (Figure 2D). As controls, we showed the absence of both peroxisome proliferator-activated receptor γ coactivator 1 (PGC1) and P53 transcription factors in the protein complexes bound to both probes (Figure 2D).

Finally, S1T induction was shown to occur through the PERK-eIF2α-ATF4 pathway, since RNAi-driven knockdown of PERK ($PERK_{RNAi}$) significantly reduced eIF2α phosphorylation and abrogated S1T induction upon BFA treatment (Figure 2E, upper panel). $Control_{RNAi}$ transfection did not modify PERK-mediated eIF2α phosphorylation in BFA-treated cells (Figure 2E, lower panel).

S1T Expression Links ER Stress to Deregulation of ER Ca^{2+} Homeostasis

We have previously shown that S1T triggers Ca^{2+} leak by forming homodimers in the ER membrane and depletes the ER Ca^{2+} pool (Chami et al., 2001). Here we showed, by using cytosolic and ER-targeted recombinant aequorin probes, that similarly to S1T, ER stressors (20 hr of treatment) induced a reduction of steady-state ER [Ca^{2+}] ($[Ca^{2+}]_{er}$) and agonist-evoked cytosolic Ca^{2+} peak ($[Ca^{2+}]_{cyt}$) (Figures 3A and S3A; Tables S1 and S2). We deliberately used a concentration of SERCA inhibitors that does not provide complete inhibition of the SERCA, to study the effect of S1T on ER Ca^{2+} content and leak. Note also that the decreased agonist-evoked cytosolic Ca^{2+} signal observed in S1T-transfected cells is largely due to the decreased $[Ca^{2+}]_{er}$, since no modification of extracellular Ca^{2+} influx was observed (Figure S3B).

Interestingly, BFA treatment for 2 hr induced the expression of the endogenous S1T and a parallel decrease of $[Ca^{2+}]_{er}$, while neither S1T induction nor $[Ca^{2+}]_{er}$ decrease were observed after 20 min of treatment (Figures 3B and 3C). These results suggest that S1T is likely to be involved in ER Ca^{2+} depletion upon ER stress.

Indeed, analyses of ER Ca^{2+} homeostasis in cells subjected to different ER stressors after knockdown of S1T expression revealed that BFA-, TBU-, and TG-induced reduction of ER Ca^{2+} steady state and subsequent agonist-evoked cytosolic signal were significantly reverted by $S1T_{RNAi}$ (Figures 3D and S3C; Tables S1 and S2). Decreased $[Ca^{2+}]_{er}$ was demonstrated to be likely due to increased ER Ca^{2+} leakage (Figures S4A and S4B). In addition, ER Ca^{2+} pool was progressively depleted upon S1T expression (Table S1), indicating that S1T-dependent ER Ca^{2+} leak is persistent over time. Control tests showed that (1) $S1T_{RNAi}$ but not $Control_{RNAi}$ transfection reversed the reduction of $[Ca^{2+}]_{er}$ induced by S1T overexpression, and (2) $S1T_{RNAi}$ did not modify the increased $[Ca^{2+}]_{er}$ induced by SERCA2b overexpression (Figure S2C; Table S1).

All in all, these data demonstrate that ER Ca^{2+} depletion upon ER stress is mediated by S1T.

S1T Is Localized to Mitochondria-Associated Membranes and Determines Mitochondrial Immobilization and Docking at the ER Surface

We then showed by using western blot and subcellular fractionation that S1T (endogenous and upon ectopic expression) is enriched both in the microsomal (Mic) and the mitochondria-associated membrane (MAM) fractions (Figure 4A). Accordingly, high-resolution imaging demonstrated that S1T colocalized with mitochondria (Figure 4B). This finding suggests that S1T-dependent ER Ca^{2+} leak may preferentially occur in the ER-mitochondria microdomains.

It was recently shown that elevated Ca^{2+} signals in microdomains between mitochondria and ER Ca^{2+} release sites immobilize mitochondria close to the ER, thus increasing ER-mitochondria physical association (Brough et al., 2005; Yi et al., 2004). We then applied time-lapse imaging of the mitochondrial network and 3D-digital microscopy to quantify mitochondrial movements and ER-mitochondria colocalization, respectively. BFA treatment (3 hr) as well as S1T overexpression (40 hr) were shown to induce inhibition of mitochondrial movements (Figure 4C; Table S3) and to increase the extent of association between ER and mitochondria (Figure 4D). These effects were reverted in BFA-treated cells by $S1T_{RNAi}$ (Figure 4C; Table S3) and upon Ca^{2+} chelation by BAPTA-AM in both BFA-treated and S1T-overexpressing cells (Figures 4C and 4D).

Interestingly, docking of mitochondria to the ER was shown to occur in S1T but not in SERCA1-expressing cells and to increase progressively upon S1T expression (Figure 4D).

Finally, reduction of ER-mitochondria distance was also demonstrated by transmission electron microscopy in S1T and S1T-GFP-transfected cells for 40 hr as compared to control cells (Figure 4E).

These data allowed us to identify S1T as a protein of the ER-mitochondria contact sites that controls mitochondrial movement and docking to the ER in a Ca^{2+}-dependent manner.

ER Stress Increases Ca^{2+} Transfer to Mitochondria through S1T Induction

Since MAM regulate Ca^{2+} signaling between ER and mitochondria (Hajnoczky et al., 2000; Rizzuto et al., 1993), S1T may play a role at MAM in regulating Ca^{2+} signaling between these two organelles.

Analysis of basal mitochondrial Ca^{2+} load by using X-rhod-1, AM dye, showed that S1T overexpression (8 hr) as well as BFA treatment (20 hr) determined a huge increase of basal mitochondrial Ca^{2+} level, which was corrected by $S1T_{RNAi}$ transfection in BFA-treated cells (Figure 5A; Table S4). Furthermore, no modification of resting cytosolic Ca^{2+} level (as measured with fluo-4, AM dye) was observed 8 hr post S1T transfection (Table S2), arguing that S1T-dependent Ca^{2+} leak occurs preferentially in the ER-mitochondria contact sites.

These microdomains constitute a preferential pathway leading to mitochondrial Ca^{2+} accumulation upon Ca^{2+} release by IP_3 receptor (Rizzuto et al., 1993).

Indeed, S1T transfection (8 hr) and BFA treatment (20 hr) led to a vast increase of agonist-evoked mitochondrial Ca^{2+} accumulation ($[Ca^{2+}]_{mt}$) as measured with mitAEQ probe, which was corrected by $S1T_{RNAi}$ transfection in BFA-treated cells (Figure 5B; Table S4).

No modification of agonist-evoked $[Ca^{2+}]_{cyt}$ was observed in S1T-transfected cells 8 hr posttransfection (Table S2), indicating that S1T-dependent increased ER-mitochondria apposition enhances IP_3-mediated Ca^{2+} transfer to mitochondria, leading to increased mitochondrial signals in stimulated cells.

Long-term expression of S1T (40 hr post-S1T-transfection) determined a reduction of basal and agonist-evoked mitochondrial Ca^{2+} load (Figures 5A and 5B; Table S4). Under these conditions, we observed a significant alteration of mitochondrial network, which was reverted by BAPTA-AM treatment (Figure 5C), while mitochondrial structure was mostly tubular-like (normal) 8 hr post-S1T-transfection (Figure 5C).

Accordingly, simultaneous evaluation of Ca^{2+} uptake rate and mitochondrial structure in single cells by using mitochondria-targeted pericam probe and digital imaging, performed 40 hr after S1T transfection, allowed us to identify two different cell populations: (1) cells with tubular-like mitochondrial network and a higher Ca^{2+} uptake rate and amplitude [S1T(T), 20%], and (2) cells with an altered mitochondrial network and a lower Ca^{2+} uptake rate and amplitude [S1T(A), 80%] (Figure 5D; Table S5).

These data suggest that mitochondrial structure alteration and decreased Ca^{2+} content follow mitochondria Ca^{2+} overload.

S1T Overexpression and ER Stress Induce Ca^{2+}-Dependent Apoptosis through the Mitochondrial Gateway

As mitochondrial Ca^{2+} overload is one of the major factors triggering mitochondrial apoptosis (Kroemer et al., 2007), we lastly investigated the involvement of S1T protein in the activation of mitochondrial apoptotic pathway upon ER stress induction. We assumed that mitochondrial apoptosis is a late effect of S1T expression and thus performed experiments 40 hr after

transfection of S1T. First, by using digital imaging and 3D reconstitution, we showed that mitochondrial volume (a parameter of mitochondrial swelling), but not ER volume, was significantly increased in S1T-overexpressing cells as compared to control and SERCA1-overexpressing cells (Figure 6A). Mitochondrial swelling induced by S1T was further confirmed by transmission electron microscopy as demonstrated by increased mitochondrial cross-section area (Figure 6B). A decrease of mitochondrial potential ($\Delta\Psi_m$) (TMRM intensity) was also noticed in S1T-GFP-transfected cells as compared to control and SERCA1-GFP-overexpressing cells (Figure 6C). Moreover, the loss of $\Delta\Psi_m$ was accompanied by the mitochondrial release of cytochrome *c* in S1T-transfected cells as compared to control cells (low and diffuse versus high and compartmentalized cytochrome *c* signal) (Figure 6D). We then demonstrated that S1T overexpression induced two specific hallmarks of apoptosis, the cleavage of caspase-3 and poly (ADP-ribose) polymerase (PARP), which were blocked by the application of the pan-caspase inhibitor ZVAD-fmk (Figure 6E). Lastly, S1T-related cell death was significantly abolished by ZVAD-fmk, BAPTA-AM, and the inhibitor of mitochondrial permeability transition pore cyclosporin A (CsA). Interestingly, no cumulative effect was observed with ZVAD-fmk and BAPTA-AM cotreatment (Figure 6F). No effect on the viability of SERCA1-overexpressing cells was noted with the same treatments (Figure 6F). These findings indicate that S1T overexpression leads to mitochondria-mediated apoptosis bearing all the principal features of the process and that this is driven by both mitochondrial Ca^{2+} overload and caspase activation.

If S1T induction took part in ER stress signaling, we would expect that stress conditions evoke the same apoptotic pathway. Indeed, BFA treatment for 20 hr, apart from inducing increased mitochondrial Ca^{2+} accumulation (Figures 5A and 5B), also led to apoptotic changes analogous to S1T, i.e., mitochondrial network alterations and swelling (Figures 7A and 7B), cytochrome *c* release (Figure 7C), translocation of proapoptotic factor Bax to the mitochondria (Figure 7D), and cleavage of caspase-3 and PARP (Figure 7E). Importantly, BFA-induced changes were reverted by $S1T_{RNAi}$ or by BAPTA-AM (Figures 7A-7E). Finally, we demonstrated that silencing of S1T significantly reduced apoptosis mediated by ER stressors (Figure 7F). As control we showed that these drugs used in the same conditions did not induced necrotic cell death (Figure 7F, inset). Overall, these data pointed out the key role of S1T in the control of ER stress-related apoptosis.

DISCUSSION

This work provides evidence that the SERCA1 truncated variant (S1T) promotes cell death through ER stress amplification, CHOP activation, ER-mitochondria Ca^{2+} transfer, and Ca^{2+}-driven sensitization of the mitochondrial apoptotic pathway (Figure S5).

Throughout this study we disclosed the mechanisms underlying the induction of S1T under ER stress conditions. Kinetic changes of the expression profiles of known ER stress signaling components and S1T revealed that S1T is induced early through the PERK-eIF2α-ATF4 pathway. Full-length SERCA1 was not induced under ER stress, suggesting that this regulation occurred in a spliced variant-specific manner. Interestingly, increase of SERCA2b isoform expression and activity has already been reported in cells subjected to drug-induced ER stress (Caspersen et al., 2000; Hojmann Larsen et al., 2001). Since S1T and SERCA2b have opposite effects on $[Ca^{2+}]_{er}$, the balanced expression of both Ca^{2+} transporters is expected to be finely tuned during ER stress to keep cell fate under control. Accordingly, induction of SERCA2b and calreticulin as well as GRP78 is likely to enable protein translation during chronic ER stress through sufficient ER Ca^{2+} storing capacity and reduction of PERK-dependent translation inhibition, respectively (Brostrom and Brostrom, 2003).

Furthermore, our data demonstrated that S1T achieves a positive feedback on the PERK-eIF2α-ATF4 pathway, since eIF2α phosphorylation and CHOP activation upon BFA treatment were drastically reduced by S1T silencing. Recently, it was shown that excessive phosphorylation of eIF2α potentiates fatty-acid-induced ER stress and subsequent apoptosis in pancreatic b cells (Cnop et al., 2007) and that ATF4-mediated CHOP induction leads to cell-cycle arrest and/or apoptosis (Oyadomari and Mori, 2004). Finally, BH3-only Bcl-2 family members (Bim, Puma, and Noxa) have been recently identified as ER stress-related apoptotic effectors downstream of CHOP and P53 activation (Li et al., 2006; Puthalakath et al., 2007). It appears that, in ER stress signaling, S1T acts early as a key component of the proapoptotic cascade, downstream of ATF4 and in concert with CHOP, to control the lethal outcome of ER stressed cells.

We show here that S1T expression leads to a progressive depletion of ER Ca^{2+} pool. Since S1T is localized within the ER-mitochondria contact sites and determines Ca^{2+} leak, we assume that S1T-dependent Ca^{2+} leak occurs within these sites channeling leaky Ca^{2+} toward the mitochondria. As a consequence, basal mitochondrial Ca^{2+} level increases upon S1T expression.

It has been previously reported that Ca^{2+} regulates both mitochondrial motility and association between mitochondria and ER (Brough et al., 2005; Wang et al., 2000; Yi et al., 2004). Accordingly, we showed that S1T induces mitochondria immobilization in a Ca^{2+}-dependent manner and leads to a progressive increase of ER-mitochondria connections. Moreover, S1T-expressing cells displayed an increased agonist-evoked mitochondrial Ca^{2+} signals. These results are in agreement with recent studies demonstrating that ER-mitochondria contacts are increased under ER stress conditions (Csordas et al., 2006; Tiwari et al., 2006) and that IP_3-mediated Ca^{2+} transfer toward mitochondria is enhanced by stable interaction between these organelles (Filippin et al., 2003) and upon artificial linkage between the ER and the outer mitochondrial membranes (Csordas et al., 2006).

Recent studies highlighted that chaperone machinery at both mitochondria and ER sides (grp75 and Sigma-1R, respectively) regulate IP_3R-mediated mitochondrial Ca^{2+} signaling through the stabilization of IP_3R on ER-mitochondria contact sites (Hayashi and Su, 2007; Szabadkai et al., 2006). Further studies would be deserved in order to determine if S1T interacts with chaperones or Ca^{2+} proteins located within ER-mitochondria contacts.

Artificial increase of ER-mitochondria contacts led to Ca^{2+}-induced cell death in rat peritoneal mast cells (Csordas et al., 2006), while depletion of PACS-2, maintaining ER-mitochondria contacts, conferred resistance to apoptosis (Simmen et al., 2005). As S1T expression persists during ER stress, mitochondrial Ca^{2+} signals decrease as a consequence of mitochondrial Ca^{2+} overload-induced mitochondrial permeabilization and swelling (Kroemer et al., 2007).

Finally, it is noteworthy that both proapoptotic S1T and antiapoptotic Bcl-2 proteins induce ER Ca^{2+} leak. Unlike S1T, Bcl-2, which has never been shown to be located at MAM, was found to reduce mitochondrial Ca^{2+} uptake (Pinton et al., 2000) and to inhibit mitochondrial Ca^{2+} waves preceding apoptosis (Magnelli et al., 1994).

Overall, we identified S1T as a key molecular player in ER stress-related apoptosis. Since ER stress has been identified as a common physiopathological process in a number of major diseases, our finding are expected to promote future research avenues with potential clinical impact.

EXPERIMENTAL PROCEDURES

Additional information regarding cell culture, plasmids, transient transfection, aequorin measurements, protein preparation, western blot, imaging, electron microscopy, search for putative sites for transcriptions factors, and cellular viability and death analyses can be found in the Supplemental Data.

Inhibition of PERK and S1T Protein Expression

PERK/EIF2AK3 (Hs_EIF2AK3_5 HP Validated siRNA) ($PERK_{RNAi}$) was purchased from QIAGEN SA. HeLa cells were exposed to RNAi for 48 hr using HiPerFect Transfection Reagent (QIAGEN SA) according to the manufacturer's instructions. GripNA oligo (peptide nucleic acid, Active Motif) was used for S1T knockdown experiments. $S1T_{RNAi}$: 5′-AGCTAGAGCGGCCTCCAT-3′. $Control_{RNAi}$ (5′-ATGGAGGCCGCTCATGCT-3^0) was used as a negative control. Tagged $S1T_{RNAi}$ (Fluorescein-$S1T_{RNAi}$) was used in imaging experiments to identify RNAi-transfected cells. Chariot II (Active Motif) was used to transfect the gripNAs, according to the manufacturer's instructions. Transfection efficiency of $S1T_{RNAi}$ was estimated to 40%. For aequorin measurements, cells were transfected first with aequorin and then with $S1T_{RNAi}$. By using this protocol, $S1T_{RNAi}$ was shown to be efficiently transfected (~40%) in aequorin-expressing cells (Figure S2D).

Aequorin Measurements

Cytosolic, mitochondrial, and ER Ca^{2+} analyses were performed by using aequorin-targeted probes. For details see the Supplemental Experimental Procedures.

Imaging Analyses

Morphological, Ca^{2+} imaging, and mitochondrial potential analyses were performed as previously described (Szabadkai et al., 2004) (Supplemental Experimental Procedures). For measurement of mitochondrial movements, images were acquired on a Zeiss LSM 510 confocal microscope (Carl Zeiss) after loading cells with 10 nM Mitotracker Red CMX Ros in KRB/Ca^{2+} at 37 C for 15 min. Time-series images were taken with a time interval of 10 s between each image. Images were 2D deconvolved, median filtered, thresholded, and clipped to 8 bit binary images using Metamorph (Universal Imaging) software. Using the stack-T-functions/Delta-F-down plugin of the WCIF ImageJ software (http://www.uhnres.utoronto.ca/facilities/wcif/), pixels in each frame were subtracted from the next frame. The resulting images were quantified by measuring the total area of object on the binary and ΔF images by the Integrated Morphometry Analysis function of the Metamorph software. Data were normalized as the ratio of ΔF area values over the total area of the original binary images for each cell. This parameter is referred to as the mitochondrial movement index (MI). Binarization and normalization were applied to avoid artifacts eventually arising from changes of intensity and focal plane.

Protein Preparation and Western Blot Analyses

Total and microsomal protein preparation and subcellular fractionation were performed as previously described (Chami et al., 2001; Vance, 1990) (Supplemental Experimental Procedures). Protein loading was normalized as compared to actin signal. Band intensity was quantified versus a control sample (arbitrarily assessed as 1), using ImageJ software.

EMSA and Oligonucleotide Pull-Down Assay

Nuclear extracts were purified as already described (Ma et al., 2002). EMSA was performed by using the LightShift Chemiluminescent EMSA Kit (Pierce). Nuclear extract (10 μg) was incubated with 20 fmol of biotin-labeled probe (Supplemental Experimental Procedures) in a

nondenaturing buffer containing 1 μg/μl poly dI•dC and 1 μg/μl poly dA•dT. Reaction mix was electrophoresed in a 5% polyacrylamide-TBE gel and transferred to a nylon membrane, and biotin signal was detected. Specificity of the reaction was assessed using 200x excess of nonlabeled probe. The oligonucleotide pull-down assay was achieved with 250 μg of nuclear extracts and 1 μg of biotin-labeled probe. DNA-protein complexes were captured on immobilized neutravidin beads (Pierce), then washed and separated by SDS-PAGE. Western blot analyses were performed on nuclear extracts and on pull-down complexes.

Statistical Analyses

Results are reported from at least three different experiments. Statistical analyses were performed using a Student's t test. A p value ≤ 0.05 was considered to be significant. All data are reported as means ± standard error of the mean (SEM).

Supplementary Material

Refer to Web version on PubMed Central for supplementary material.

ACKNOWLEDGMENTS

We thank Dr. B. Arbeille for transmission electron microscopy (EM) acquisition and analyses, Dr. C. Besmond for expert assistance in promoter analyses, and D. Lagorce for technical help. EM was performed in Cell Biology-EM Laboratory, Faculty of Medicine, Tours, France. Imagery was performed in imaging core facilities of Jacques Monod Institute, Paris VI University, Pasteur institute (PFID), Necker-Enfants Malades hospital, Paris V University, France, Telethon imagery Center, Ferrara University, Italy. Some of the pericam experiments were performed in the laboratory of Prof. M.R. Duchen, University College London, United Kingdom. This work was supported by grants from INSERM to P.P.-B. and AFM (11456 and 13291) and FRM (DEQ20071210550) to P.P.-B. and M.C., and by Telethon-Italy, the Italian Association for Cancer Research (AIRC), the Italian University Ministry (PRIN, FIRB, and local research grants), the Emilia-Romagna PRRIITT program, the Ferrara Objective 2 funds, and the Italian Space Agency (ASI) to R.R. M.C., G.S., and B.O. were supported, respectively, by an INSERM young researcher contract, an INSERM postdoctoral fellowship “poste vert,” and “Ecole de l'INSERM.”

REFERENCES

Benali-Furet NL, Chami M, Houel L, De Giorgi F, Vernejoul F, Lagorce D, Buscail L, Bartenschlager R, Ichas F, Rizzuto R, Paterlini-Brechot P. Hepatitis C virus core triggers apoptosis in liver cells by inducing ER stress and ER calcium depletion. Oncogene 2005;24:4921–4933. [PubMed: 15897896]

Berridge MJ, Lipp P, Bootman MD. The versatility and universality of calcium signalling. Nat. Rev. Mol. Cell Biol 2000;1:11–21. [PubMed: 11413485]

Bobe R, Bredoux R, Corvazier E, Lacabaratz-Porret C, Martin V, Kovacs T, Enouf J. How many Ca(2)+ATPase isoforms are expressed in a cell type? A growing family of membrane proteins illustrated by studies in platelets. Platelets 2005;16:133–150. [PubMed: 16011958]

Boyce M, Yuan J. Cellular response to endoplasmic reticulum stress: a matter of life or death. Cell Death Differ 2006;13:363–373. [PubMed: 16397583]

Brostrom MA, Brostrom CO. Calcium dynamics and endoplasmic reticular function in the regulation of protein synthesis: implications for cell growth and adaptability. Cell Calcium 2003;34:345–363. [PubMed: 12909081]

Brough D, Schell MJ, Irvine RF. Agonist-induced regulation of mitochondrial and endoplasmic reticulum motility. Biochem. J 2005;392:291–297. [PubMed: 15982187]

Caspersen C, Pedersen PS, Treiman M. The sarco/endoplasmic reticulum calcium-ATPase 2b is an endoplasmic reticulum stress-inducible protein. J. Biol. Chem 2000;275:22363–22372. [PubMed: 10748035]

Chami M, Gozuacik D, Lagorce D, Brini M, Falson P, Peaucellier G, Pinton P, Lecoeur H, Gougeon ML, le Maire M, et al. SERCA1 truncated proteins unable to pump calcium reduce the endoplasmic reticulum calcium concentration and induce apoptosis. J. Cell Biol 2001;153:1301–1314. [PubMed: 11402072]

Cnop M, Ladriere L, Hekerman P, Ortis F, Cardozo AK, Dogusan Z, Flamez D, Boyce M, Yuan J, Eizirik DL. Selective inhibition of EIF2alpha dephosphorylation potentiates fatty acid-induced endoplasmic reticulum stress and causes pancreatic beta-cell dysfunction and apoptosis. J. Biol. Chem 2007;282:3989–3997. [PubMed: 17158450]Published online December 8, 2006

Csordas G, Renken C, Varnai P, Walter L, Weaver D, Buttle KF, Balla T, Mannella CA, Hajnoczky G. Structural and functional features and significance of the physical linkage between ER and mitochondria. J. Cell Biol 2006;174:915–921. [PubMed: 16982799]

Deniaud A, Sharaf El Dein O, Maillier E, Poncet D, Kroemer G, Lemaire C, Brenner C. Endoplasmic reticulum stress induces calcium-dependent permeability transition, mitochondrial outer membrane permeabilization and apoptosis. Oncogene 2008;27:285–299. [PubMed: 17700538]Published online August 13, 2007

Ferreiro E, Costa R, Marques S, Cardoso SM, Oliveira CR, Pereira CM. Involvement of mitochondria in endoplasmic reticulum stress-induced apoptotic cell death pathway triggered by the prion peptide PrP(106-126). J. Neurochem 2008;104:766–776. [PubMed: 17995926]Published online November 6, 2007

Filippin L, Magalhaes PJ, Di Benedetto G, Colella M, Pozzan T. Stable interactions between mitochondria and endoplasmic reticulum allow rapid accumulation of calcium in a subpopulation of mitochondria. J. Biol. Chem 2003;278:39224–39234. [PubMed: 12874292]

Hajnoczky G, Csordas G, Madesh M, Pacher P. The machinery of local Ca2+ signalling between sarco-endoplasmic reticulum and mitochondria. J. Physiol 2000;529:69–81. [PubMed: 11080252]

Hayashi T, Su TP. Sigma-1 Receptor Chaperones at the ERMitochondrion Interface Regulate Ca(2+) Signaling and Cell Survival. Cell 2007;131:596–610. [PubMed: 17981125]

Hetz C, Bernasconi P, Fisher J, Lee AH, Bassik MC, Antonsson B, Brandt GS, Iwakoshi NN, Schinzel A, Glimcher LH, Korsmeyer SJ. Proapoptotic BAX and BAK modulate the unfolded protein response by a direct interaction with IRE1alpha. Science 2006;312:572–576. [PubMed: 16645094]

Hojmann Larsen A, Frandsen A, Treiman M. Upregulation of the SERCA-type Ca2+ pump activity in response to endoplasmic reticulum stress in PC12 cells. BMC Biochem 2001;2:4. [PubMed: 11319943]

Kroemer G, Galluzzi L, Brenner C. Mitochondrial membrane permeabilization in cell death. Physiol. Rev 2007;87:99–163. [PubMed: 17237344]

Li J, Lee B, Lee AS. Endoplasmic reticulum stress-induced apoptosis: multiple pathways and activation of p53-up-regulated modulator of apoptosis (PUMA) and NOXA by p53. J. Biol. Chem 2006;281:7260–7270. [PubMed: 16407291]

Luo S, Baumeister P, Yang S, Abcouwer SF, Lee AS. Induction of Grp78/BiP by translational block: activation of the Grp78 promoter by ATF4 through and upstream ATF/CRE site independent of the endoplasmic reticulum stress elements. J. Biol. Chem 2003;278:37375–37385. [PubMed: 12871976]

Ma Y, Brewer JW, Diehl JA, Hendershot LM. Two distinct stress signaling pathways converge upon the CHOP promoter during the mammalian unfolded protein response. J. Mol. Biol 2002;318:1351–1365. [PubMed: 12083523]

Magnelli L, Cinelli M, Turchetti A, Chiarugi VP. Bcl-2 overexpression abolishes early calcium waving preceding apoptosis in NIH-3T3 murine fibroblasts. Biochem. Biophys. Res. Commun 1994;204:84–90. [PubMed: 7945396]

Ohoka N, Yoshii S, Hattori T, Onozaki K, Hayashi H. TRB3, a novel ER stress-inducible gene, is induced via ATF4-CHOP pathway and is involved in cell death. EMBO J 2005;24:1243–1255. [PubMed: 15775988]

Oyadomari S, Mori M. Roles of CHOP/GADD153 in endoplasmic reticulum stress. Cell Death Differ 2004;11:381–389. [PubMed: 14685163]

Pinton P, Ferrari D, Magalhaes P, Schulze-Osthoff K, Di Virgilio F, Pozzan T, Rizzuto R. Reduced loading of intracellular Ca(2+) stores and downregulation of capacitative Ca(2+) influx in Bcl-2-overexpressing cells. J. Cell Biol 2000;148:857–862. [PubMed: 10704437]

Pizzo P, Pozzan T. Mitochondria-endoplasmic reticulum choreography: structure and signaling dynamics. Trends Cell Biol 2007;17:511–517. [PubMed: 17851078]

Puthalakath H, O'Reilly LA, Gunn P, Lee L, Kelly PN, Huntington ND, Hughes PD, Michalak EM, McKimm-Breschkin J, Motoyama N, et al. ER stress triggers apoptosis by activating BH3-only protein Bim. Cell 2007;129:1337–1349. [PubMed: 17604722]

Rizzuto R, Brini M, Murgia M, Pozzan T. Microdomains with high Ca2+ close to IP3-sensitive channels that are sensed by neighboring mitochondria. Science 1993;262:744–747. [PubMed: 8235595]

Rizzuto R, Pinton P, Ferrari D, Chami M, Szabadkai G, Magalhaes PJ, Di Virgilio F, Pozzan T. Calcium and apoptosis: facts and hypotheses. Oncogene 2003;22:8619–8627. [PubMed: 14634623]

Schroder M, Kaufman RJ. The mammalian unfolded protein response. Annu. Rev. Biochem 2005;74:739–789. [PubMed: 15952902]

Simmen T, Aslan JE, Blagoveshchenskaya AD, Thomas L, Wan L, Xiang Y, Feliciangeli SF, Hung CH, Crump CM, Thomas G. PACS-2 controls endoplasmic reticulum-mitochondria communication and Bid-mediated apoptosis. EMBO J 2005;24:717–729. [PubMed: 15692567]

Szabadkai G, Simoni AM, Chami M, Wieckowski MR, Youle RJ, Rizzuto R. Drp-1-dependent division of the mitochondrial network blocks intraorganellar Ca2+ waves and protects against Ca2+-mediated apoptosis. Mol. Cell 2004;16:59–68. [PubMed: 15469822]

Szabadkai G, Bianchi K, Varnai P, De Stefani D, Wieckowski MR, Cavagna D, Nagy AI, Balla T, Rizzuto R. Chaperone-mediated coupling of endoplasmic reticulum and mitochondrial Ca2+ channels. J. Cell Biol 2006;175:901–911. [PubMed: 17178908]

Szegezdi E, Logue SE, Gorman AM, Samali A. Mediators of endoplasmic reticulum stress-induced apoptosis. EMBO Rep 2006;7:880–885. [PubMed: 16953201]

Tiwari M, Kumar A, Sinha RA, Shrivastava A, Balapure AK, Sharma R, Bajpai VK, Mitra K, Babu S, Godbole MM. Mechanism of 4-HPR-induced apoptosis in glioma cells: evidences suggesting role of mitochondrial-mediated pathway and endoplasmic reticulum stress. Carcinogen-esis 2006;27:2047–2058.

Vance JE. Phospholipid synthesis in a membrane fraction associated with mitochondria. J. Biol. Chem 1990;265:7248–7256. [PubMed: 2332429]

Vangheluwe P, Raeymaekers L, Dode L, Wuytack F. Modulating sarco(endo)plasmic reticulum Ca2+ ATPase 2 (SERCA2) activity: cell biological implications. Cell Calcium 2005;38:291–302. [PubMed: 16105684]

Wang HJ, Guay G, Pogan L, Sauve R, Nabi IR. Calcium regulates the association between mitochondria and a smooth subdomain of the endoplasmic reticulum. J. Cell Biol 2000;150:1489–1498. [PubMed: 10995452]

Yi M, Weaver D, Hajnoczky G. Control of mitochondrial motility and distribution by the calcium signal: a homeostatic circuit. J. Cell Biol 2004;167:661–672. [PubMed: 15545319]

Yoshida H, Haze K, Yanagi H, Yura T, Mori K. Identification of the cis-acting endoplasmic reticulum stress response element responsible for transcriptional induction of mammalian glucose-regulated proteins. Involvement of basic leucine zipper transcription factors. J. Biol. Chem 1998;273:33741–33749. [PubMed: 9837962]

Zhang Y, Fujii J, Phillips MS, Chen HS, Karpati G, Yee WC, Schrank B, Cornblath DR, Boylan KB, MacLennan DH. Characterization of cDNA and genomic DNA encoding SERCA1, the Ca(2+)-ATPase of human fast-twitch skeletal muscle sarcoplasmic reticulum, and its elimination as a candidate gene for Brody disease. Genomics 1995;30:415–424. [PubMed: 8825625]

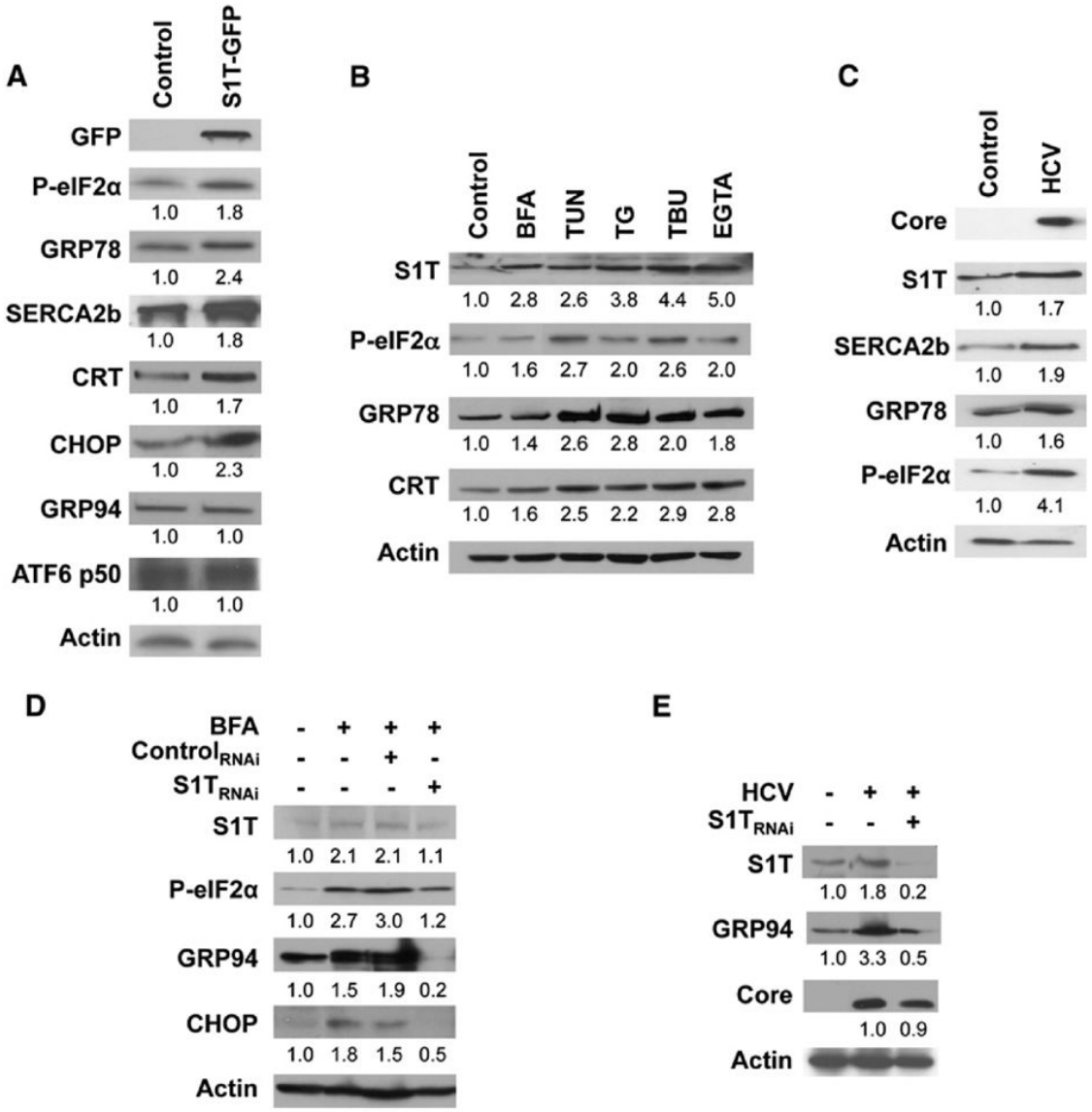

Figure 1. S1T Is an ER Stress Protein

(A) Detection of ER stress proteins (phosphorylated alpha-subunit of eukaryotic Initiation Factor 2 [P-eIF2α], GRP78, SERCA2b, Calreticulin [CRT], CHOP, GRP94, and ATF6 p50) in pcDNA3.1 (Control) or S1T-GFP-transfected HeLa cells for 40 hr. (B and C) Expression of endogenous S1T and of ER stress proteins in HeLa cells treated for 20 hr with 5 μg/ml BFA, 10 μg/ml TUN, 0.5 μM TG, 10 μM TBU, or 2 mM EGTA (B), and in hepatitis C virus "replicon" (HCV) and in control cell lines. (C) HCV core antibody was used as control. (D and E) Detection of S1T and of ER stress proteins in HeLa cells treated or not treated with 0.5 μg/ml BFA for 20 hr (D) and in HCV "replicon" cells (E) transfected or not transfected with $S1T_{RNAi}$ or $Control_{RNAi}$.

S1T, S1T-GFP, and SERCA2b were detected on microsomal fraction in (A) and (C) and in total extracts in (B), (D), and (E). All the other proteins were detected on total extracts. GFP antibody was used to detect S1T-GFP protein.

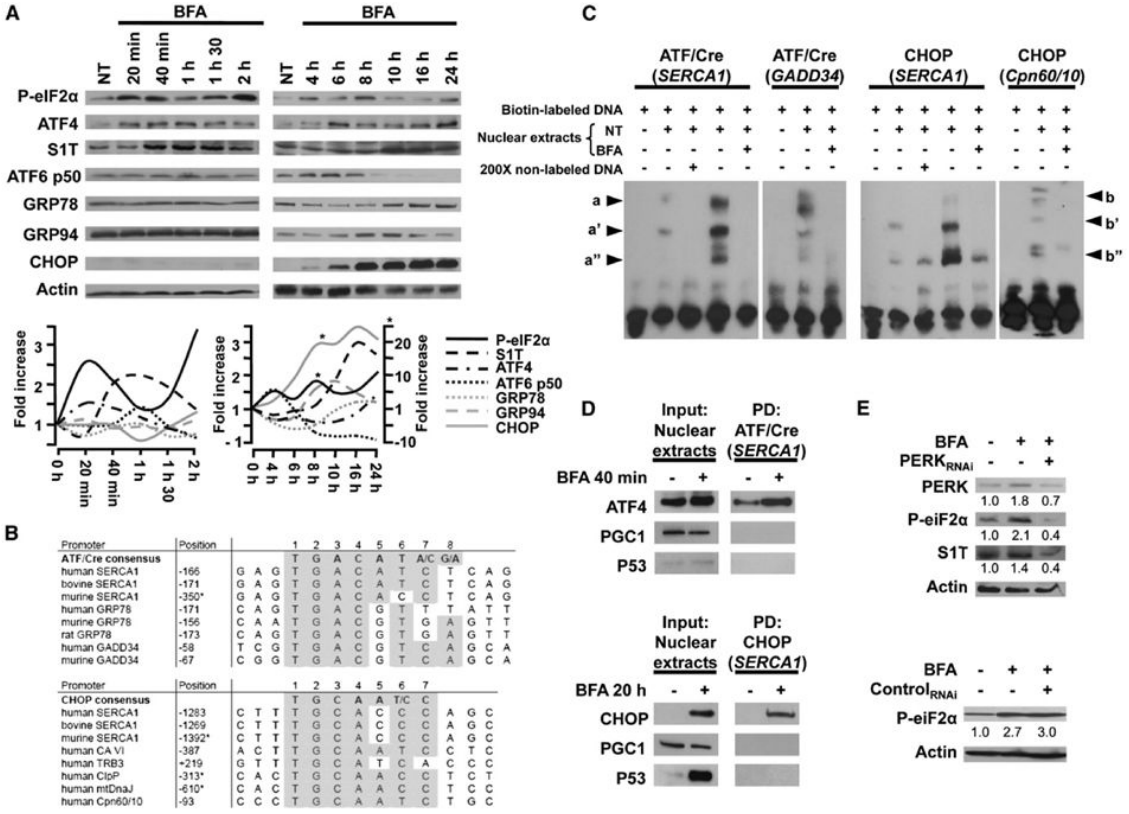

Figure 2. S1T Is Induced through the PERK-eIF2α-ATF4 Pathway

All the experiments were performed in HeLa cells treated or not treated with 0.5 μg/ml BFA.

(A) Induction of S1T and of ER stress proteins in cells treated for the indicated time points. Graphs: time course induction. Where indicated (asterisk), traces are referring to right scale.

(B) (Upper panel) Alignment of ATF/Cre-responsive element found in *SERCA1*, *GRP78*, and *Growth Arrest and DNA Damage-inducible protein 34* (*GADD34*) genes. (Lower panel) Alignment of CHOP-responsive element found in *SERCA1*, *carbonic anyhdrase VI* (*CA VI*), *tribbles-related protein 3 (TRB3)*, *caseinolytic serine protease* (*ClpP*), *mitochondrial heat shock protein DnaJ* (*mtDnaJ*), and *chaperonins 60/10* (*Cpn 60/10*) genes. The base positions of the consensus are shaded and indicated 5′→3′. Positions are relative to transcription start site or where indicated (asterisk) to initiation codon.

(C) Electrophoresis mobility shift assay with ATF/Cre and CHOP probes derived from the *SERCA1*, the *GADD34*, and the *Cpn60/10* promoters performed on nuclear extracts from cells left nontreated (NT) or treated with BFA for 40 min (for ATF/Cre probes) or 20 hr (for CHOP probes). The shifted ATF4 and CHOP complexes are indicated by arrows a, a′, and a″ and b, b′, b″, respectively.

(D) Oligonucleotide pull-down assay with biotin-labeled probes used in (C), and western blot analyses of DNA-protein complexes in nuclear extracts (input) and on pull-down complexes (PD).

(E) Detection of PERK, P-eIF2α, and S1T in HeLa cells treated or not treated with 0.5 μg/ml BFA for 1 hr transfected or not transfected with $Control_{RNAi}$ or $PERK_{RNAi}$. In (A) and (E), total extracts were used for western blot analyses.

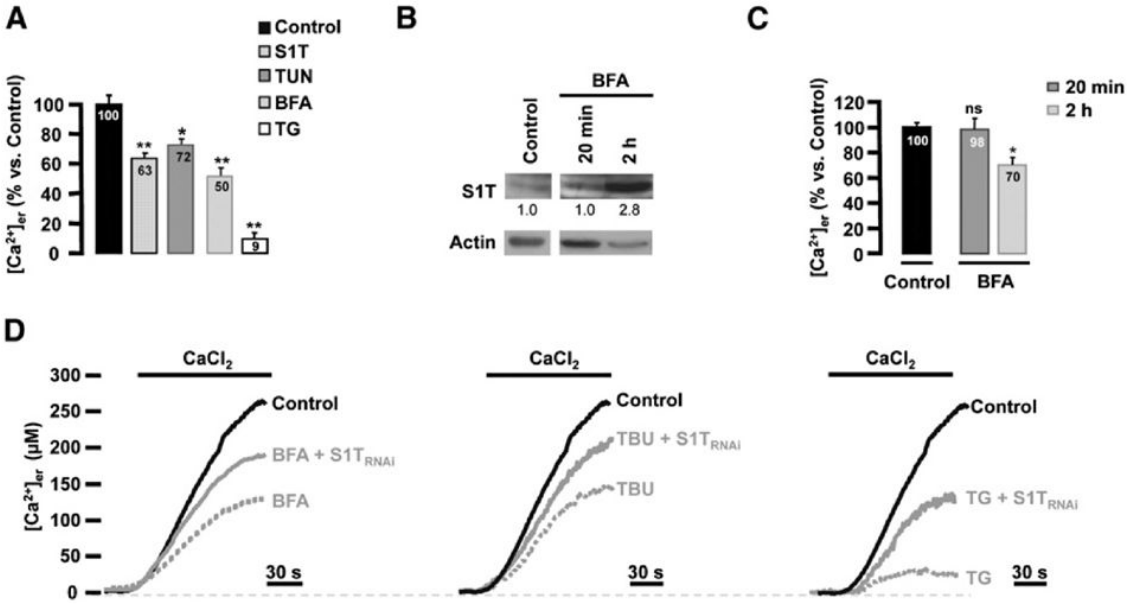

Figure 3. S1T Mediates Ca^{2+} Deregulation Related to ER Stress

In (A), (C), and (D), $[Ca^{2+}]_{er}$ was measured using erAEQ probe 40 hr posttransfection. (A and C) Steady-state $[Ca^{2+}]_{er}$ (presented as a percentage of control considered as 100%) in nontreated HeLa cells (Control), 0.5 μg/ml BFA, 1 μg/ml TUN, 2.5 nM TG-treated cells for 20 hr, in S1T-pcDNA3.1-transfected cells for 40 hr (S1T) (A) (Student's t test, *$p < 0.05$, **$p < 0.005$ versus Control) and in nontreated HeLa cells (Control), in BFA-treated cells for 20 min or 2 hr (Student's t test, ns = nonsignificant, *$p < 0.005$ versus Control) (C). (B) Expression of S1T in HeLa cells treated with 0.5 μg/ml BFA for the indicated time points. (D) Representative traces of $[Ca^{2+}]_{er}$ in nontreated HeLa cells (Control) and in 0.5 μg/ml BFA, 10 μM TBU, or 2.5 nM TG-treated cells for 20 hr transfected or not transfected with $S1T_{RNAi}$. The effect of $S1T_{RNAi}$ was recorded in 40% of aequorintransfected cells and thus underestimated (see the Experimental Procedures). Data in (A), (C), and (D) are represented as mean ± SEM. Numbers of experiments are indicated in Table S1.

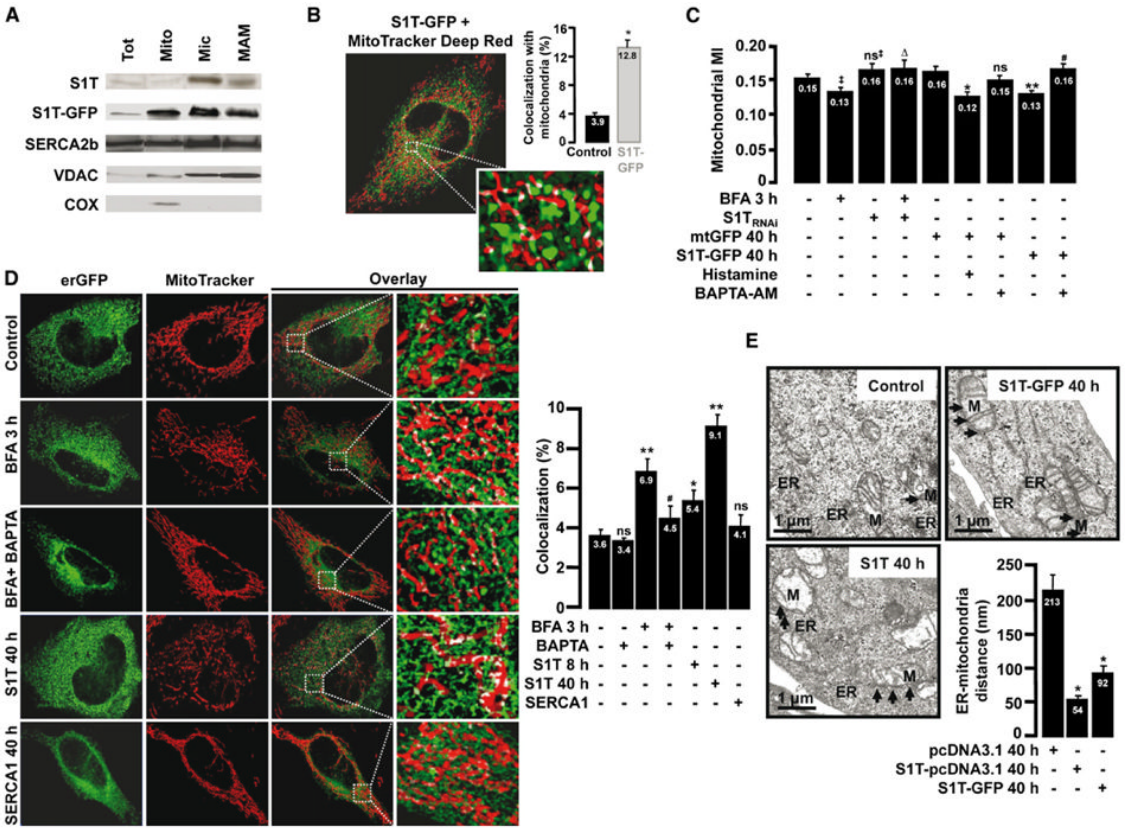

Figure 4. S1T Is Localized to Mitochondria-Associated Membranes and Determines Mitochondrial Immobilization and Docking at the ER Surface

(A) Subcellular fractionation. Tot, total; mito, crude mitochondria; Mic, microsomes; MAM, mitochondrial-associated membranes. All endogenous proteins except S1T-GFP were detected in nontransfected HeLa cells. S1T and GFP antibodies were used to detect endogenous S1T and S1T-GFP 40 hr posttransfection, respectively. SERCA2b, VDAC, and cytochrome *c* oxydase (COX) were used as microsomal, MAM, and mitochondrial fractions markers, respectively.

(B) Quantification of colocalization of S1T with mitochondria (labeled with MitoTracker Deep Red) in living HeLa cells transfected with S1T-GFP (S1T-GFP, n = 20) or with erGFP probe (Control, n = 10). Representative magnified image shows S1T-GFP signal in green, mitochondria in red, and colocalization in white. Student's t test, *$p < 0.0005$ versus Control.

(C) Mitochondrial movements analyzes in HeLa cells treated with 0.5 µg/ml BFA (3 hr) transfected or not transfected with $S1T_{RNAi}$-fluorescein or transfected with mtGFP or S1T-GFP. In $S1T_{RNAi}$ conditions, quantification was performed exclusively in $S1T_{RNAi}$-fluorescein-positive cells. Mitochondrial movements was evaluated before and after 100 µM histamine stimulation (used as control of ER Ca^{2+} release-related mitochondrial immobilization) or upon BAPTA-AM (5 µM, 20 hr) application. Student's t test, $ns^{‡}$ = nonsignificant, $^{‡}p < 0.005$ versus nontreated cells, $^{Δ}p < 0.005$ versus BFA-treated cells, ns* = nonsignificant, *$p < 0.05$, and **$p < 0.0005$ versus mtGFP-transfected cells, $^{#}p < 0.0005$ versus S1T-transfected cells. Numbers of experiments are indicated in Table S3.

(D) Graph: quantitative analysis of the colocalization of ER and mitochondria (as percentage of total mitochondrial volume) in HeLa cells cotransfected with erGFP and S1T-pcDNA3.1 (S1T 8 hr, n = 16; S1T 40 hr, n = 11) or SERCA1-pcDNA3.1 (SERCA1, n = 9) or in cells transfected with erGFP left untreated (Control, n = 30) or treated with 5 µM BAPTA-AM for 3 hr (Control + BAPTA-AM, n = 17) or with 0.5 µg/ml BFA (BFA, n = 19), or with BFA and

BAPTA-AM (BFA + BAPTA-AM, n = 8). Representative images of ER (erGFP, green), mitochondria (MitoTracker Deep Red, red) and magnified overlay images showing colocalization between ER and mitochondria (white). Student's t test, ns = nonsignificant, *$p < 0.005$, **$p < 0.0005$ versus Control, and $^{\#}p < 0.05$ versus BFA.

(E) Representative fields of electron micrographs and ER-mitochondria distance (graph) in HeLa cells transfected for 40 hr with pcDNA3.1, S1T-pcDNA3.1, or S1T-GFP (Control, n = 31; S1T, n = 46; S1T-GFP, n = 44). M, mitochondria; ER, endoplasmic reticulum. Arrows indicate proximity of ER to mitochondria. Student's t test, *$p < 0.0005$ versus Control.

Data in (B)-(E) are represented as mean ± SEM.

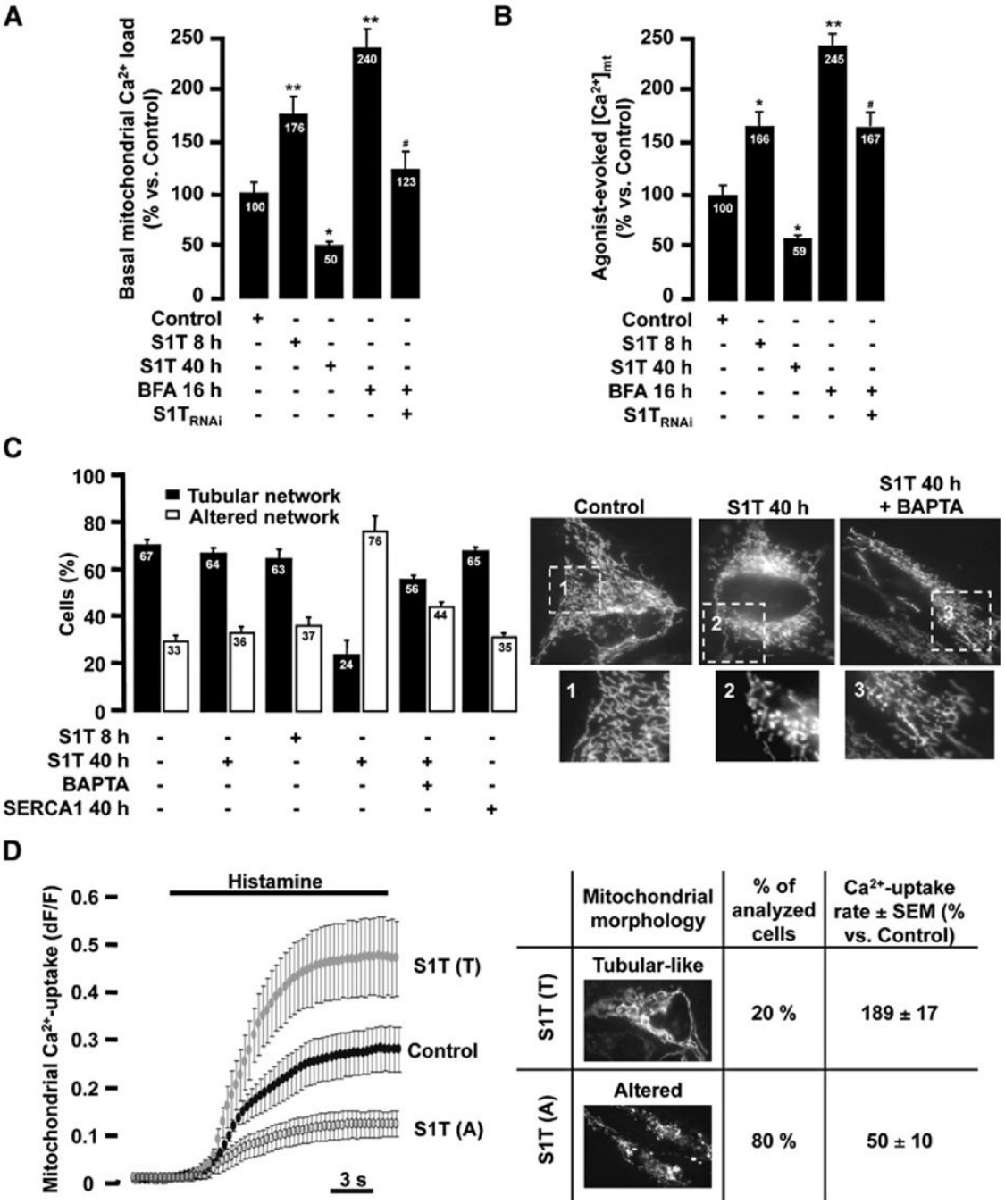

Figure 5. S1T Overexpression Enhances Basal and Agonist-Evoked Mitochondrial Ca^{2+} Load, Leading to Mitochondrial Structure Alteration

(A) Mitochondrial basal Ca^{2+} level as evaluated with X-rhod-1, AM dye in HeLa cells transfected with S1T-pcDNA3.1 (S1T) for 8 hr and 40 hr or in cells treated with 0.5 μg/ml BFA for 20 hr and transfected or not transfected with $S1T_{RNAi}$. Calibrated values of basal mitochondrial Ca^{2+} load are presented as percentages of controls (pcDNA3.1-transfected or nontreated cells) considered as 100%. The effect of $S1T_{RNAi}$ was recorded in $S1T_{RNAi}$-positive cells (fluorescein-positive cells). Values of basal mitochondrial Ca^{2+} level are provided in μM in Table S4 and were determined as described in the Supplemental Experimental Procedures. Student's t test, $^{*}p < 0.01$, $^{**}p < 0.0001$ versus Control, $^{\#}p < 0.005$ versus BFA.

(B) Mitochondrial agonist-evoked Ca^{2+} uptake (peak value) after 100 μM histamine application, as measured with mitAEQmut probe, in HeLa cells transfected or treated as in (A), and presented as percentage of controls considered as 100%. The effect of $S1T_{RNAi}$ was recorded in 40% of aequorin-transfected cells and thus underestimated. Student's t test, *$p < 0.005$, **$p < 0.0001$ versus Control, $^{\#}p < 0.005$ versus BFA.

(C) Percentage of cells with tubular mitochondrial network and those with altered mitochondrial network in HeLa cells (see representative images) cotransfected with mitBFP and pcDNA3.1 (Control, n = 58) or S1T-GFP (S1T 8 hr, n = 83; S1T 40 hr, n = 105) or SERCA1-GFP (SERCA1, n = 50) and in Control and S1T cells (40 hr) treated with 5 μM BAPTA-AM for 20 hr posttransfection (n = 64 and n = 74, respectively).

(D) Relative fluorescence intensity changes (dF/F) following 100 μM histamine stimulation in HeLa cells 40 hr after cotransfection of mitochondrial pericam probe and pcDNA3.1 (Control) or S1T-pcDNA3.1 [S1T(T) with tubular-like mitochondrial network and S1T(A) with altered mitochondrial network]. Table: representative images of the mitochondrial network of S1T (T) and (A) cells, percentage of each population, and maximal rate of mitochondrial Ca^{2+} uptake evaluated from the ascending phase of dF/F kinetics versus Control considered as 100%. The Control trace shows the mean ± SEM of cells with tubular versus altered mitochondrial network (Table S5). Data in (A)-(D) are represented as mean ± SEM. For (A), (B), and (D), numbers of experiments are indicated in Tables S4 and S5.

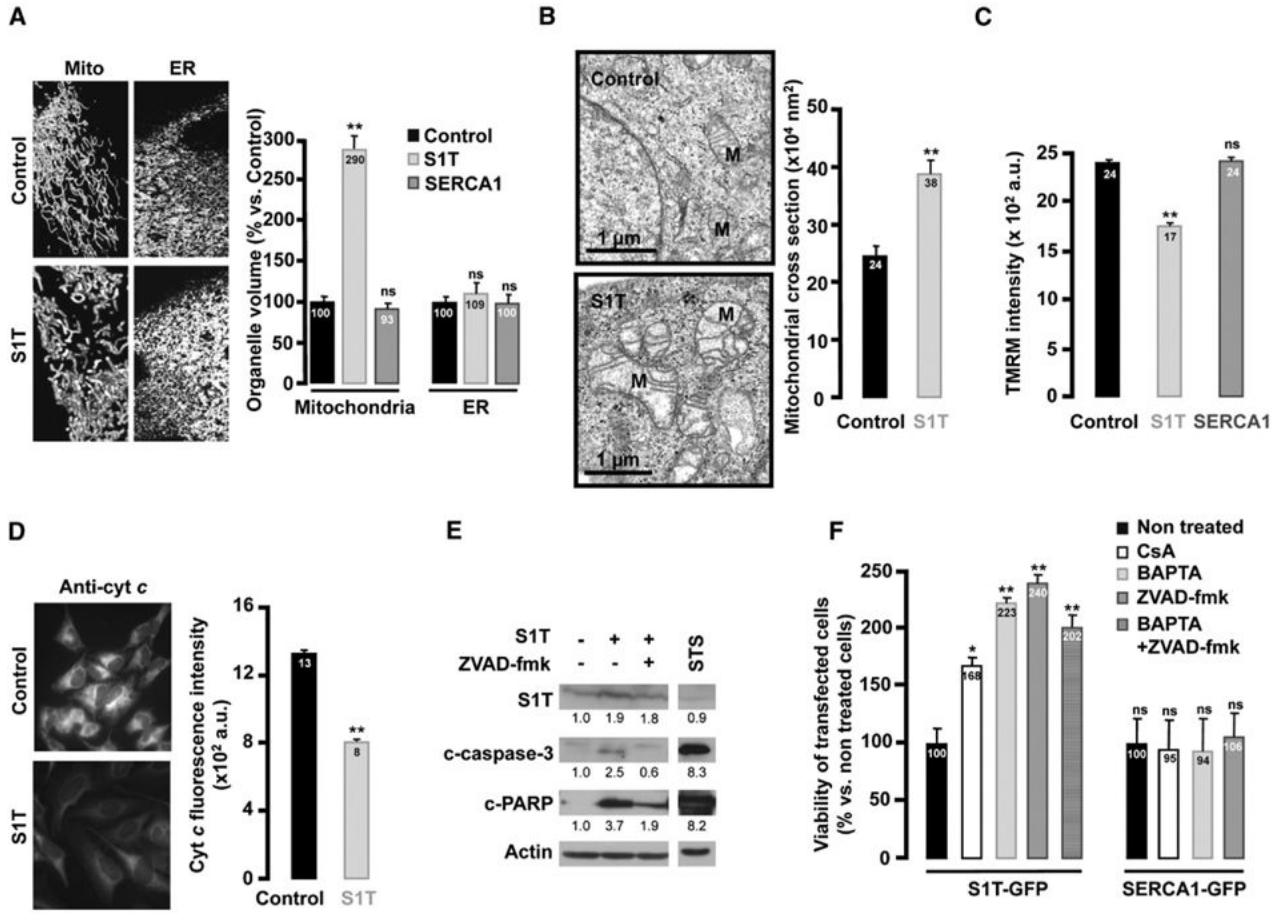

Figure 6. S1T Alters Mitochondrial Structure and Function

All these analyses were performed in HeLa cells 40 hr posttransfection. (A) Representative high-magnification 3D-reconstructed images of cells transfected as described in Figure 4D. Mitochondrial and ER volume were evaluated (as compared to Control cells considered as 100%) (Control, n = 18; S1T, n = 18; SERCA1, n = 10). (B) Representative fields of electron micrographs of cells transfected with pcDNA3.1 (Control, n = 109) or with S1T-pcDNA3.1 (S1T, n = 110). M, mitochondria. Graph: mean of mitochondria cross-sectional area. (C) Mitochondrial potential change was evaluated after transfection of GFP empty vector (Control, n = 326), S1T-GFP (S1T, n = 155), or SERCA1-GFP (SERCA1, n = 201). (D) Representative images and graph showing cytochrome *c* fluorescence intensity in cells transfected with pcDNA3.1 (Control, n = 262) or S1T-GFP (S1T, n = 189). (E) Western blot analyses of cells transfected with pcDNA3.1 or with S1T-pcDNA3.1 and treated or not treated with 100 µM ZVAD-fmk for 20 hr. As positive control, cells were treated with 1 µM staurosporine (STS) for 2 hr. (F) Cellular viability in S1T-GFP or SERCA1-GFP-overexpressing cells treated (20 hr posttransfection) or not treated with 12 µg/ml cyclosporine A (CsA), 5 µM BAPTA-AM, and 100 µM ZVAD-fmk, presented as percentages of GFP-fluorescent cells among the whole cell population (determined by Hoechst staining) versus the nontreated transfected cells considered as 100%. Student's t test, ns = nonsignificant, *p < 0.05, and **p < 0.0005 versus Control. Data are represented as mean ± SEM.

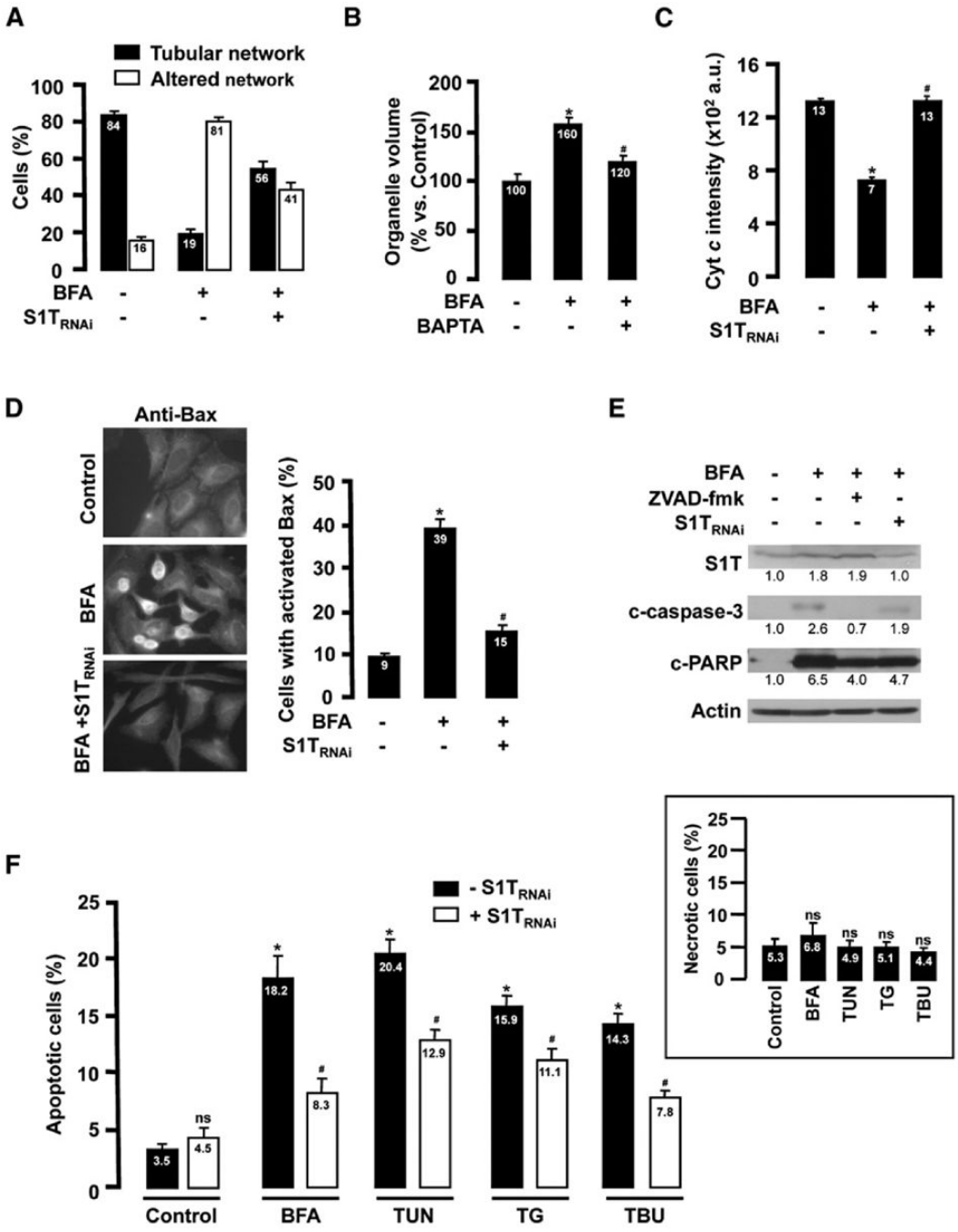

Figure 7. S1T Knockdown Reduces BFA-Induced Apoptosis

All the experiments were performed in HeLa cells left untreated or treated with 0.5 μg/ml BFA for 20 hr and transfected or not transfected with S1T$_{RNAi}$. (A) Percentage of cells with tubular or altered mitochondrial network in Control (n = 428), BFA (n = 293), and BFA + S1T$_{RNAi}$ (n = 197) cells. (B) Mitochondrial volume recorded as in Figure 6A in Control (n = 19), in BFA (n = 24), and in BFA cells cotreated with 5 μM BAPTA-AM (BFA + BAPTAAM; n = 12). (C) Quantification of cytochrome *c* fluorescence intensity evaluated as in Figure 6D in Control (n = 262), in BFA (n = 335), and in BFA + S1T$_{RNAi}$ (n = 242) cells. (D) Percentage of cells with activated Bax (intense mitochondrial staining in representative images) in Control (n = 747), BFA (n = 596), and BFA + S1T$_{RNAi}$ cells (n = 300). (E) Western blot analyses

performed as in Figure 6E. (F) Percentage of apoptotic bodies in nontreated cells (Control) or treated for 20 hr with 0.5 μg/ml BFA, 5 μg/ml TUN, 0.5 μM TG, and 10 μM TBU after being transfected or not transfected with $S1T_{RNAi}$. Inset: Percentage of necrotic cells (propidium-iodide-positive cells) recorded in the same conditions. (A, E, and F) Effect of $S1T_{RNAi}$ is recorded in total cell population and thus underestimated. (C and D) Quantification was performed exclusively in $S1T_{RNAi}$-fluorescein-positive cells. (B-D and F) Student's t test, ns = nonsignificant, $^{*}p < 0.0001$ versus Control, $^{\#}p < 0.0001$ versus BFA, TUN, TG, or TBU. Data are represented as mean ± SEM.